Measurement of nitrogen monoxide levels in gas flows with a micro total analytical system based on LTCC

Thomas Geiling, Tilo Welker, Heike Bartsch & Jens Müller
Department of Electronics Technology
Ilmenau University of Technology
Gustav-Kirchhoff-Str. 5, 98693 Ilmenau, Germany
E-Mail: thomas.geiling@tu-ilmenau.de

Abstract

The measurement of nitrogen monoxide (NO) concentration levels is a vital aspect of environmental analysis and the so called CHNS analysis. The chemiluminescent reaction with ozone in the gas phase is a well-established method for the measurement of atmospheric concentration levels in the range from 4 ppb up to 100 ppm.
In this contribution we present the design of a so called micro total analytical system (µTAS) for NO measurements designed in ceramic. Low temperature co-fired ceramics (LTCC) have proven to be the ideal technology, since they offer high chemical and thermal stability as well as high degree of freedom of design. The article gives an overview of the design process with emphasis on manufacture of the components and technological challenges regarding life-time.

Introduction

The measurement of nitrogen oxides is an integral part of the combustion analysis or so called CHNS-analysis, which is applied in order to determine the elemental composition of organic and inorganic compounds. The measurement principle is based on the complete combustion of a sample in an oxygen rich atmosphere, during which the compounds are decomposed and the released chemical elements are oxidized. Subsequently, the fraction of each oxide, CO_2, H_2O, N_2, NO, NO_2, and SO_2, is determined, and a variety of different measurement methods exists for each oxide. With the fraction of each oxide known, the molecular formula of the combusted sample can be deduced. CHNS analyzers are used extensively in a wide range of applications, including analysis of oil and oil-related products as well as food products, [1].
In this contribution we present an approach for the design and manufacture of a device capable of measuring low to medium NO concentrations in gases at atmospheric pressure. The objective of the development is a module, consisting of all necessary components connected via microfluidic channels inside a common substrate, which can be integrated into a CHNS analytical system. Further, the module may be assembled in a handheld device alone, which can be utilized for environmental analysis.
Low temperature co-fired ceramics (LTCC) were chosen as substrate material, since they offer high chemical and thermal stability as wells as high degree of freedom of design. Of the available LTCC tape systems DP 951 by DuPont offers the highest degree of freedom for manufacturing microfluidic systems, [2; 3].
The article gives an overview of the design and highlights some aspects of fabrication. The main focus is on the microfluidic system. Hence, the sensor electronics as well as the power electronics are omitted.

Measurement principle

The analysis of the chemiluminescent reaction of nitrogen monoxide with ozone (O_3) has proven to be one of the most sensitive procedures for the measurement of NO concentration levels. Since the method enables a high sampling rate and provides very good linearity within the range of atmospheric NO concentrations from 4 ppb up to 100 ppm, it is widespread for these kinds of measurements, [4]. Further, measurements in the ppt-range with this method have also been reported, [5]. *Fontijn et al.* have shown that the interference with low concentrations of other common components of ambient air, such as NO_2, CO_2, CO, NH_3, SO_2, and hydrocarbons, is negligible, [6]. The characteristic reaction of NO with O_3 is given in equations (1) and (2).

$$NO + O_3 \rightarrow NO_2^* \quad (1)$$

$$NO_2^* \rightarrow NO_2 + h\upsilon \quad (2)$$

The excited nitrogen dioxide emits a distinctive broadband spectrum ranging from 600 nm up to a wavelength of 2600 nm with a maximum in the near infrared around 1200 nm, [7]. Usually, the infrared emission near the maximum is measured.

Overall design

From the measurement principle one can deduce the essential components, which make up the microfluidic set-up of the micro total analytical system (µTAS). The schematical layout is depicted in figure 1.

Ozone generator. Since ozone cannot be stored without considerable effort, the predominant approach is to create ozone on-site from oxygen or dried air in a dielectric barrier discharge.

CLD Reaction chamber. The generated ozone is brought into contact with the analyte gas carrying the unknown levels of NO inside a reaction chamber or so called chemiluminescence detection (CLD) chamber. A viewport enables the collection of the emitted radiation with a photo diode.

Exhaust gas treatment. In order to achieve good linearity, the chemiluminescent reaction must not affect the ozone concentration considerably. This implicates, that a large quantity of ozone needs to be generated and only small amounts of this quantity are consumed during the chemiluminescent reaction. The large excess needs to be purged, before the gas mixture can be exhausted into the environment.

As shown in figure 1, the substrate also includes the microfluidic channels, the fluidic ports to the surrounding CHNS analyzer, and the gas mixer, which is located in front of the CLD chamber.

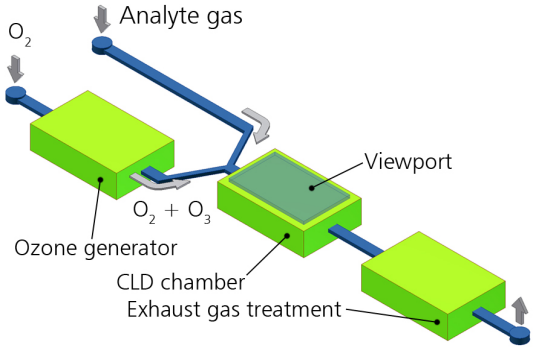

Figure 1. Schematical layout of the µTAS design

Ozone generator

Design. A classical approach to generate ozone is the dielectric barrier discharge (DBD) or silent discharge. A high voltage, either AC or DC, is applied between two parallel planar electrodes, of which at least one is covered with a dielectric in order to prevent arcing. The ozone is produced within the coronas of the filamentary discharges from dissociated oxygen and molecular oxygen, [8].

In contrast to this classical setup, all electrodes can be arranged at the bottom of a channel. *Baker et al.* as well as *Pavón* realized a horizontal or planar setup, where the gas flows parallel to the layers on which structured electrodes are screen printed, [10; 11]. The setup is depicted on the left side of figure 2.

The advantage of this horizontal assembly is the straightforward fabrication of the ozone generator combined with the possibility to test its functionality without burying the device inside a substrate. Additionally, this setup is assumed to operate at lowered breakdown voltage due to peaks in the electric field distribution.

According to Paschen's Law, one either needs to apply a high voltage or bring the electrodes close together to initiate an electric breakdown at atmospheric pressure. Typical values for dielectric barrier discharges in air are peak-to-peak voltages V_{pp} of 3 to 20 kV and electrode distances ranging from 0.2 mm up to 5 mm, [9].

LTCC technology combined with screen printing technique enables electrode distances well below 1 mm. Hence, a lower exciting voltage can be selected. For the ozone generator, a custom built AC generator with a V_{pp} of 7 kV at a constant frequency of 30 kHz is used. The applied power is tuned via an overlying pulse-width modulation which controls the power-on time.

Further, the horizontal setup was adapted in order to maximize the ozone generation rate. The driven electrode and the mass electrode are positioned on the same layer. The layout is depicted on the right side of figure 2. This arrangement maximizes the ozone generation rate, since significantly more ozone is produced in the negative corona of the discharge, [12]. Otherwise, like in the setup depicted on the left side of figure 2, every second half-cycle only a positive corona is initiated in the gas flow.

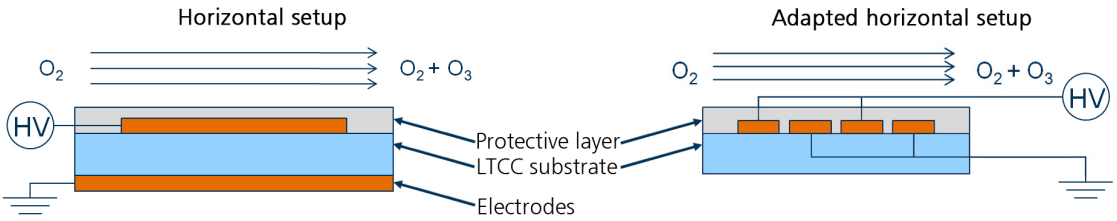

Figure 2. Horizontal setup for a LTCC discharge device, as proposed in [10; 11], and adapted setup for improved ozone yield

A selection of realized ozone generators is depicted in figure 3. The footprint of the LTCC substrate amounts to 58 x 19.4 mm². The top electrodes are 1 mm wide, 40 mm long, and structured with various additional noses in order to amplify the electric field peaks. They also increase the length of the edges of the electrode, where the dielectric discharge takes place. The bottom electrode, which is not shown in the picture, is of rectangular shape and extends towards the edges of the substrate. The thickness of the LTCC substrate, and therefore the electrode distance is 560 µm. The electrodes are screen printed with Pd / Ag paste DP6146 by DuPont and have a thickness of approx. 12 µm. A generator with the adapted horizontal setup is depicted in figure 4. Here, the electrode distance is 250 µm.

The highly reactive species created in the discharge, such as O, and O_3, readily attack and deteriorate the electrode material. Hence, all electrodes of the ozone generator must be covered with a protective layer. With the horizontal setup, the electrodes can easily be covered by a screen printed ink or a thin ceramic layer. Therefore, this setup was chosen for the initial experiments with the ozone generator. An additional advantage of the setup is the simplified access to the protective layer for the purpose of analysis.

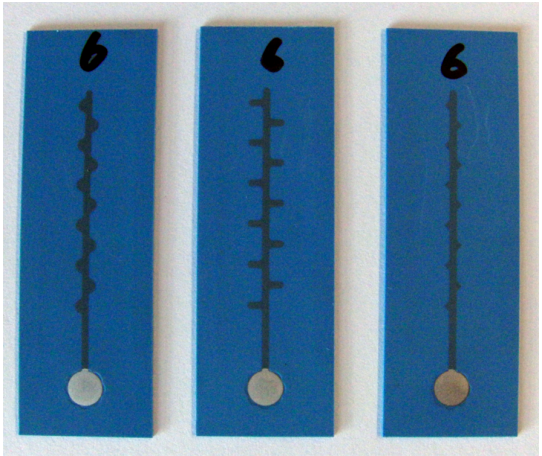

Figure 3. Picture of several ozone generators with structured top electrodes and ceramic protective layer

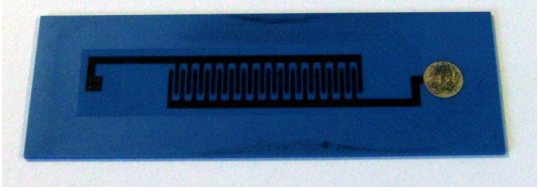

Figure 4. Top view of an ozone generator with improved horizontal setup and glass protective layer

Protective layer. Because the electrode setup will be buried inside a microfluidic channel in a following development stage, the protective layer has to be co-fired with the substrate. This means, that the electrode and the protective layer are applied in the same step. The aim of the initial set of experiments was to find a protective layer, capable of hermetically sealing the electrodes from the discharge.

To test the hermetic sealing of the protective layers the devices were dipped into a galvanic bath of copper (II) sulfate $CuSO_4$ and contacted as the cathode. A flowing current indicates a pinhole in the protective layer. Further, the galvanic test reveals the position of the pinhole, since the deposited copper is visible with the naked eye.

At first, a screen printed protective layer applied locally on the electrodes was tested. DuPont DP 9615 glass encapsulant was used, since it is compatible with the DP 951 system and promises high chemical stability. Single and double printed thick films with fired thicknesses of 12 µm and 24 µm respectively were tested. After each printing step the paste was dried for 5 min at 80 °C.

Screen printing of the protective layers did not result in a hermetically sealing. The galvanic test revealed pinholes in 5 out of 6 fabricated devices. The electrical tests showed that the pinholes are the reason for increased arcing at this location. They lead to the immediate destruction of the protective layer and the electrode beneath, as shown in figure 5.

Further analysis of the glass film revealed blistering throughout the protective film with increased amounts above the electrodes. Presumably, the overlying glass layer prevents the binder of the

electrode paste and the LTCC substrate from volatizing completely during the burnout phase. This leads to the observed cavities within the protective layer. It is assumed, that simultaneous printing of several thick films with another screen printed paste is unlikely. Therefore, this approach was not pursued further.

Instead, the potential of the ceramic substrate being employed as protective layer was examined. A thin tape of the DP 951 system was chosen. Although it is thicker than the fired glass protective layer, and therefore requires a higher breakdown voltage, manufacture of the protective layer is straight forward, since the ceramic tape is stapled and laminated with the substrate.

The sealing of the manufactured devices was also tested in the galvanic bath. All of the 32 tested protective layers proved to hermetically seal the underlying electrodes. In addition, the function tests showed no initial failure. Therefore, an endurance test was conducted. The device shown in the middle of figure 3 was operated in a sealed PTFE housing for ca. 600 h. The protective layer was then examined with a white-light interferometer Wyko NT 9300 at the tip of a nose, which is the area with the highest electric field strength. The obtained topography is depicted in figure 6. It shows trenches arranged in a honeycomb-like structure. It is assumed that due to the initial roughness of the protective layer preferential locations are formed, where the filamentary discharges strike with higher frequency. This leads to an increased local abrasion. However, only about 15 µm, which amounts to approx. 36 %, of the ceramic layer has been removed during the endurance test. Therefore, a suitable protective layer has been found, which withstands the deteriorating conditions.

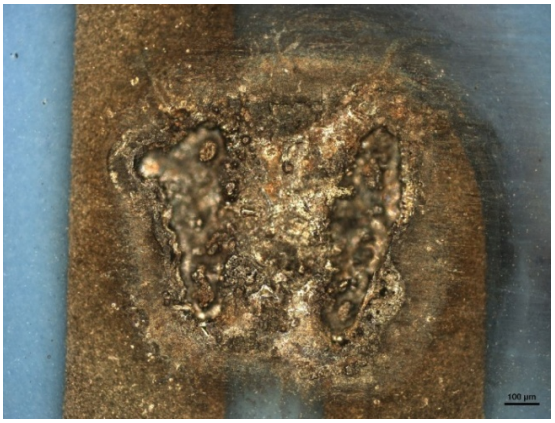

Figure 5. Micrograph of deteriorated DP 9615 glass protective layer after function test

CLD chamber

Design. The ozone is mixed with the analyte gas in a Y mixer closely arranged to the reaction chamber, in order to collect emitted radiation as soon as the reaction begins. The reaction chamber has a volume of approx. 16.8 mm³ and is covered with an IR transparent window D263T by Schott AG on which the photo diode will be positioned. The footprint of the window is 8 x 8 mm² with a thickness of 200 µm. The glass edges are used for bonding with the substrate. Therefore, an area of approx. 6 x 6 mm² is available for observation.

Fabrication process. The structures of the CLD chamber are laser cut in green LTCC sheets. Usually, the sheets are laminated together in a single step. In this case, the pressure distribution will lead to a deformation of the cavities. Therefore, the sheets were laminated together in a sequential lamination process, which is depicted schematically in figure 7. First, the respective sheets for the base, the Y mixer and the CLD chamber are laminated separately. In a second step the three fragments are laminated together with lower pressure, in order to preserve the shape of the cavities. Figure 8 shows the cross section

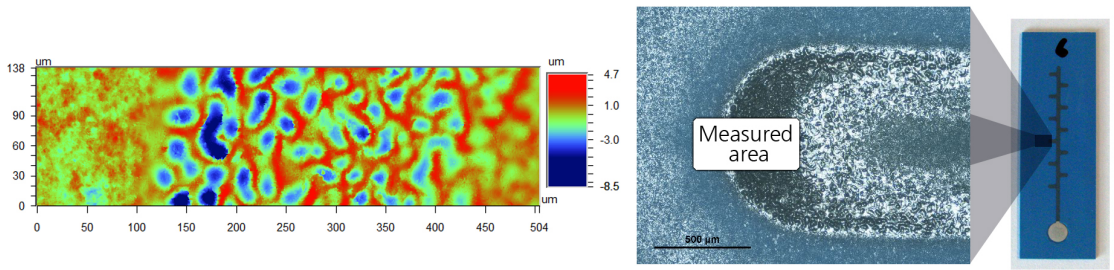

Figure 6. Topography of the area with highest electric field strength after 600 h of continuous operation

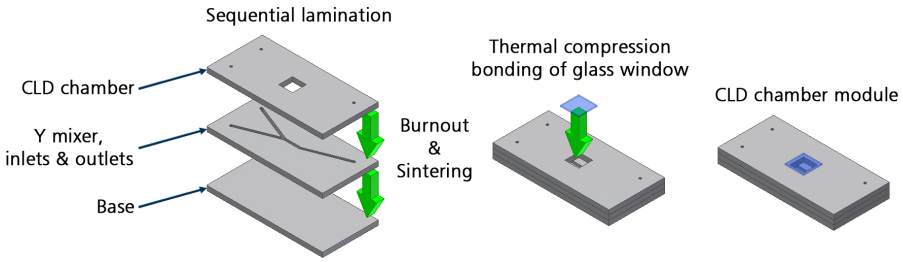

Figure 7. Schematic fabrication process of the CLD chamber with sequential lamination and thermal compression bonding of the glass window

of the fired channel of a sintered substrate.

The IR transparent window is bonded on the fired LTCC using the glass frit bonding technique. The sealing glass frits are applied in paste form on the glass window and the LTCC substrate by screen printing. After a separate burnout step, the two parts are bonded together by thermal compression bonding. The areas with the glass frit are pressed together and heated above the melting temperature. The glass frits on both parts melt and combine to a tight sealing. Figure 9 shows a manufactured CLD chamber with the bonded glass window. Of the available glass frits, several sealing glasses with low melting points under 450 °C were tested.

Sealing of the bonded interface was analyzed with a helium leak test. The CLD chamber was coupled with a helium sensitive mass spectrometer SmartTest by Pfeiffer Vacuum GmbH and evacuated to $5 \cdot 10^{-4}$ mbar. The whole substrate was then submerged in helium at atmospheric pressure. The tested sealing glass frits showed a leak rate below $5 \cdot 10^{-10}$ mbar l sec^{-1}, which implies a gas tight sealing of the CLD chamber.

Exhaust gas treatment

Design. The gas mixture leaving the reaction chamber still carries hazardous amounts of ozone and needs to be treated before it is exhausted. Ozone can be decomposed in a thermal reactor at high temperatures or by a chemical reaction with activated carbon. The use of activated carbon is ruled out, because it deteriorates during the decomposition reaction, [13]. As a consequence a replaceable exhaust gas treatment is necessary, whose integration into the LTCC substrate presents a challenge and implies additional maintenance efforts.

Therefore, thermal decomposition of ozone is preferred. In order to reduce the otherwise high temperatures above 600 °C necessary for rapid decomposition, the reaction is accelerated by a non-degrading catalyst. Of the conceivable catalyst materials, platinum is available in the form of the co-fire conductor paste DP 9896 by DuPont, which is applicable to LTCC substrates as well as to alumina substrates.

Catalyst performance. In order to estimate the performance of the catalyst and analyze the basic characteristics of the paste, samples were prepared on an alumina substrate with a footprint of 75 x 12 mm². For convenient heating, the substrates were outfitted with a resistive heater on the backside. Pictures of the substrates are shown in figure 10.

The surface are per volume has a significant influence on the performance of a catalyst. SEM analysis of the platinum surface shows a favorable micro-porous structure with a high surface area per volume. The micro-pores greatly increase the number of active sites on the Pt catalyst. A SEM picture of the micro-porous surface is depicted in figure 11.

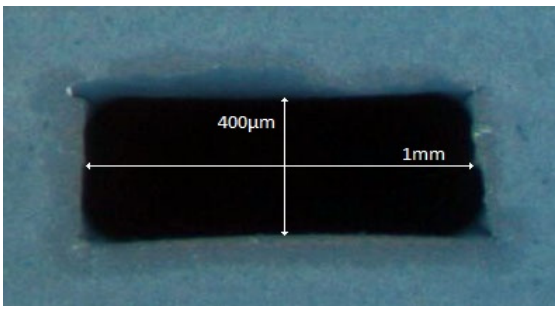

Figure 8. Cross section of a fired channel fabricated with the adapted lamination process

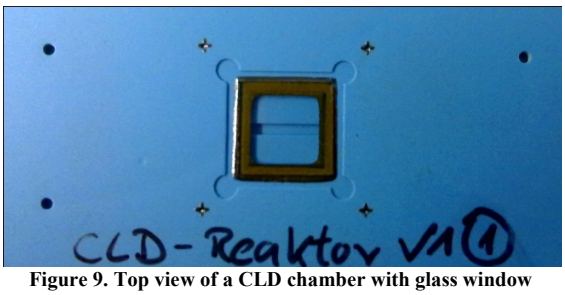

Figure 9. Top view of a CLD chamber with glass window

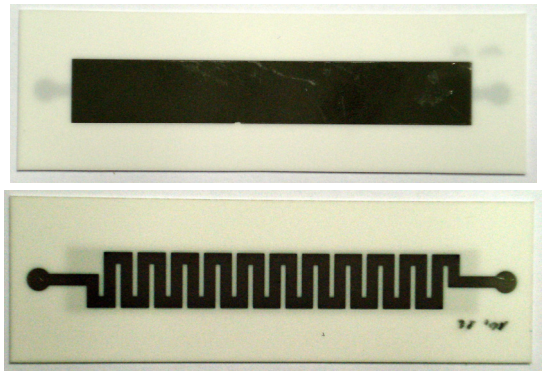

Figure 10. Photographs of the Pt catalyst on alumina substrate with resistive heater on the backside

For the performance tests the alumina substrates were given into a sealed PTFE housing with an incorporated channel. A constant flow of oxygen with an ozone concentration of approx. 5000 ppm was fed to the catalyst and the temperature was varied between room temperature and 200 °C.

Unexpectedly, catalysts which were fabricated with the same parameters initially showed different ozone decomposition characteristics. While one catalyst showed reasonable decomposition rates only at high temperatures, another catalyst already had a significant rate at room temperature. After heating the substrates to 200 °C, the effect vanished and the catalysts performed equally.

This observation led to a detailed examination of the catalysts surface chemistry. Auger electron spectroscopy (AES) revealed carbon monoxide (CO) poisoning of the Pt catalysts at varying levels. Catalysts with less CO poisoning performed better than those with higher amounts of adsorbed CO. Since the Pt catalysts were sintered on alumina substrates, the CO poisoning must have its source in the organic components of the DP 9896 paste. It is assumed, that due to the intended function as a conductor, the sintering behavior is not optimized in regard of surface chemistry.

Conclusion & outlook

The microfluidic design of a µTAS for measuring NO concentrations in gases and its essential components has been presented. The feasibility of each component, namely the ozone generator, the CLD chamber, and the exhaust gas treatment, was shown. Selected relationships between design and functional requirements have been pointed out. These are the durability of the protective layer of the ozone

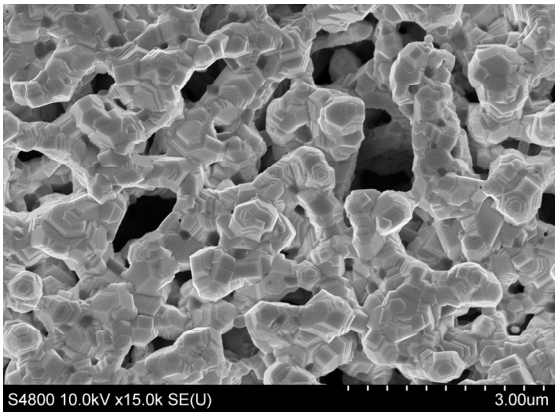

Figure 11. SEM picture of the micro-porous structure on the sintered DP 9896 paste on alumina substrate

generator and the condition of the Pt catalyst in the exhaust gas treatment.

Since all components are manufactured with the parameters according to manufacturer recommendation, the integration of all three components on a single substrate is within reach. However, management of the heat build-up on the substrate is expected to pose a challenge. Therefore, further work will concentrate on the integration, especially in view of thermal management.

Acknowledgements

The support obtained from Central Innovation Program SME (ZIM) of the Federal Ministry of Economics and Technology is gratefully acknowledged. The authors also thank their industrial partners for their unremitting support.

References

[1] Thompson, M., “amc technical briefs – CHNS Elemental Analysers”, http://www.rsc.org/images/brief%2029_tcm18-119169.pdf, accessed: 02/17/2011

[2] Thelemann, T., et al., “LTCC based fluidic components for chemical applications”, Journal of Microelectronics and Electronic Packaging, Vol. 4, No. 4, pp. 167-172, 2007.

[3] Bartsch de Torres, H., et al., “Embossing of microfluidic structures in ceramic multilayers”, Proceedings of the Smart Systems Integration Conference, pp. 423-426, Paris, March 27-28, 2007.

[4] Zhang, L. C., et al., "Recent Progress in Chemiluminescence for Gas Analysis", Applied Spectroscopy Reviews, Vol. 45, No. 6, pp. 474-489, 2010.

[5] Volz, A., et al., "Measurements of nitrogen-oxides at ppt levels by chemiluminescence with O_3", Fresenius Zeitschrift für analytische Chemie, Vol. 317, No. 3-4, pp. 355-358, 1984.
[6] Fontijn, A., et al., "Homogeneous chemiluminescent measurement of nitric oxide with ozone – Implications for continuous selective monitoring of gaseous air pollutants", Analytical Chemistry, Vol. 42, 6, 1970.
[7] Clough, P. N., et al., "Mechanism of chemiluminescent reaction between nitric oxide and ozone", Transactions of the Faraday Society, Vol. 63, pp. 915-925, 1967.
[8] Eliasson, B., et al., "Ozone synthesis from oxygen in dielectric barrier discharges", Journal of Physics D- Applied Physics, Vol. 20, No. 11, pp. 1421-1437, 1987.
[9] Wagner, H. E., et al., "The barrier discharge: basic properties and applications to surface treatment", Vacuum, Vol. 71, No. 3, pp. 417-436, 2003.
[10] Baker, A., et al., "Fabrication of a multilayered low-temperature cofired ceramic micro-plasma-generating device", International Journal of Applied Ceramic Technology, Vol. 3, No. 6, pp. 413-418, 2006.
[11] Pavón, S., "Interaction between a surface dielectric barrier discharge and transonic airflows", Dissertation, École polytechnique fédérale de Lausanne, 2008.
[12] Yehia, A., et al.," On assessment of ozone generation in dc coronas", Journal of Physics D- Applied Physics, Vol. 33, No. 7, pp. 831-835, 2000.
[13] Valdés, H., et al.," Effect of Ozone Treatment on Surface Properties of Activated Carbon", Langmuir, Vol. 18, No. 6, pp. 2111-2116, 2002.